J Nat Prod. 2021 Apr 23; 84(4): 1261–1270. PMCID: PMC8056600
Published online 2021 Apr 12. doi: 10.1021/acs.jnatprod.0c01324 PMID: 33844528

Anti-SARS-CoV-2 Activity of *Andrographis paniculata* Extract and Its Major Component Andrographolide in Human Lung Epithelial Cells and Cytotoxicity Evaluation in Major Organ Cell Representatives

Khanit Sa-ngiamsuntorn,[†#] Ampa Suksatu,[‡#] Yongyut Pewkliang,[§] Piyanoot Thongsri,[§] Phongthon Kanjanasirirat,[⊥] Suwimon Manopwisedjaroen,[‡] Sitthivut Charoensutthivarakul,[⊥∥¶] Patompon Wongtrakoongate,[¶○] Supaporn Pitiporn,[□] Jarinya Chaopreecha,[‡] Supasek Kongsomros,[‡] Kedchin Jearawuttanakul,[⊥] Warawuth Wannalo,[⊥] Phisit Khemawoot,[■] Somchai Chutipongtanate,[■●] Suparerk Borwornpinyo,[*⊥△] Arunee Thitithanyanont,[*‡] and Suradej Hongeng[⊥●]

[†]Department of Biochemistry, Faculty of Pharmacy, Mahidol University, Bangkok 10400, Thailand
[‡]Department of Microbiology, Faculty of Science, Mahidol University, Bangkok 10400, Thailand
[§]Section for Translational Medicine, Faculty of Medicine Ramathibodi Hospital, Mahidol University, Bangkok 10400, Thailand
[⊥]Excellent Center for Drug Discovery (ECDD), Faculty of Science, Mahidol University, Bangkok 10400, Thailand
[∥]School of Bioinnovation and Bio-Based Product Intelligence, Faculty of Science, Mahidol University, Bangkok 10400, Thailand
[¶]Center for Neuroscience, Faculty of Science, Mahidol University, Bangkok 10400, Thailand
[○]Department of Biochemistry, Faculty of Science, Mahidol University, Bangkok 10400,Thailand
[□]ChaoPhya Abhaibhubejhr Hospital, Prachin Buri 25000, Thailand
[■]Chakri Naruebodindra Medical Institute, Faculty of Medicine Ramathibodi Hospital, Mahidol University, Samutprakarn 10540, Thailand
[●]Department of Pediatrics, Faculty of Medicine Ramathibodi Hospital, Mahidol University, Bangkok 10400, Thailand
[△]Department of Biotechnology, Faculty of Science, Mahidol University, Bangkok 10400, Thailand
[*]Corresponding author.
[*]Tel: +66-2-201-5308. Email: bsuparerk@gmail.com.
[*]Tel: +66-2-201-5528. Email: arunee.thi@mahidol.edu.

Received 2020 Dec 8

Abstract

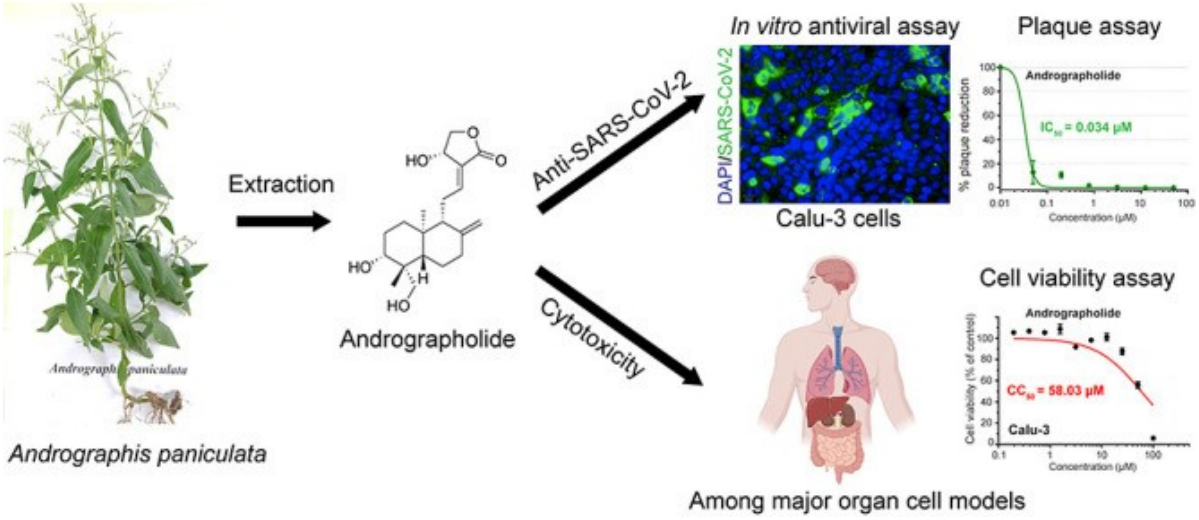

The coronaviruses disease 2019 (COVID-19) caused by a novel coronavirus (SARS-CoV-2) has become a major health problem, affecting more than 50 million people with over one million deaths globally. Effective antivirals are still lacking. Here, we optimized a high-content imaging platform and the plaque assay for viral output study using the legitimate model of human lung epithelial cells, Calu-3, to determine the anti-SARS-CoV-2 activity of *Andrographis paniculata* extract and its major component, andrographolide. SARS-CoV-2 at 25TCID$_{50}$ was able to reach the maximal infectivity of 95% in Calu-3 cells. Postinfection treatment of *A. paniculata* and andrographolide in SARS-CoV-2-infected Calu-3 cells significantly inhibited the production of infectious virions with an IC$_{50}$ of 0.036 μg/mL and 0.034 μM, respectively, as determined by the plaque assay. The cytotoxicity profile developed over the cell line representatives of major organs, including liver (HepG2 and imHC), kidney (HK-2), intestine (Caco-2), lung (Calu-3), and brain (SH-SY5Y), showed a CC$_{50}$ of >100 μg/mL for *A. paniculata* extract and 13.2–81.5 μM for andrographolide, respectively, corresponding to a selectivity index of over 380. In conclusion, this study provided experimental evidence in favor of *A. paniculata* and andrographolide for further development as a monotherapy or in combination with other effective drugs against SARS-CoV-2 infection.

The outbreak of coronavirus disease 2019 (COVID-19) is an emergent global health crisis that requires urgent solutions. Since severe acute respiratory syndrome coronavirus 2 (SAR-CoV-2) emerged in Wuhan, Hubei, China, at the end of 2019,[1] the total confirmed cases are approaching 70 million, with more than one million deaths globally at the end of December 2020. SARS-CoV-2 is a positive sense, single-stranded, enveloped RNA virus belonging to the *Coronaviridae* family and categorized as a new member of the *Betacoronavirus* genus together with severe acute respiratory syndrome coronavirus (SARS-CoV) in 2003 and Middle East respiratory syndrome coronavirus (MERS-CoV) in 2012.[2–4] The host range of SARS-CoV-2 is very broad partly due to the relative conservation of the cellular receptor, angiotensin-converting enzyme 2 (ACE2), among mammals. This phenomenon could explain the interspecies transmission of the virus from animals to cause disease in humans.[5] Even though the majority of infections were asymptomatic, clinical manifestations of COVID-19 varies widely, ranging from low-grade fever to severe pneumonia and eventually death. The outcome of the infection depended largely on host factors, e.g., age, previous health problems, and immunological status.[6–8] Among critical manifestations, acute respiratory distress syndrome, cytokine storm, and multiorgan failure are the leading causes of death in COVID-19.[9,10]

Lacking effective antivirals against SARS-CoV-2 is undoubtedly one of the main reasons of poor clinical outcomes in patients with severe COVID-19. Drug discovery and repurposing strategies are being pursued to identify potential therapeutic agents.[11−13] A beneficial instance of this effort was repositioning of remdesivir (that was originally developed for Ebola virus infection) for COVID-19 treatment.[14,15] Unfortunately, subsequent well-conducted clinical trials revealed that remdesivir had marginal clinical efficacy,[15,16] while the cost-effectiveness and accessibility are still a huge concern.[17] Therefore, further efforts should be made to identify new compounds with potent anti-SAR-CoV-2 activity. Among all promising candidates, natural products have been recognized as the major source for new drug discovery for decades.[18] Ethnobotanical evidence suggests plant-derived natural compounds are worth investigating to identify potent antivirals against coronaviruses,[19] while computational approaches have been applied for phytochemicals in order to define their target-specific antiviral potential against SARS-CoV-2.[20]

One prominent medicinal plant with various pharmacological activities is *Andrographis paniculata*, known as “king of bitters”, which belongs to the Acanthaceae family.[21] *A. paniculata* is currently used in traditional medicine to treat the common cold, diarrhea, and fever due to several infectious causes and as a health tonic.[22] A major bioactive component of *A. paniculata* is andrographolide,[23] a diterpene lactone in the isoprenoid family, which is known for its broad-spectrum antiviral properties.[24] Andrographolide was recently predicted *in silico* to have a potent anti-SARS-CoV-2 activity through specific targeting of the host ACE2 receptor and viral factors, i.e., RNA-dependent RNA polymerase, main protease, 3-CL protease, PL protease, and spike protein.[25−28] Recently, Shi et al. applied an enzyme-based assay to demonstrate an inhibitory effect of andrographolide against SARS-CoV-2 main protease (M^{pro}).[29] Furthermore, our group has utilized a phenotypic cell-based immunofluorescent assay (IFA) to reveal the anti-SARS-CoV-2 effect of *A. paniculata* extract and andrographolide in African green monkey kidney cells (Vero E6).[30] Notably the anti-SARS-CoV-2 activity of *A. paniculata* extract and andrographolide has never been elucidated in infected human lung epithelial cells.

This study aimed to evaluate the anti-SARS-CoV-2 activity of *A. paniculata* extract and its major component, andrographolide, by using a legitimate model of infected human lung epithelial cell, Calu-3.[31] Cytotoxic profiles of *A. paniculata* extract and andrographolide over five major human organs, including lung, brain, liver, kidney, and intestine, were achieved by a panel of cell line representatives. The results demonstrated that *A. paniculata* extract and andrographolide have a potent anti-SARS-CoV-2 activity with a high safety margin for major organs in cell culture models.

Results and Discussion

Optimization of Human Lung Epithelial Cells (Calu-3)-Based Anti-SARS-CoV-2 Assay

Urgent demands for effective anti-SARS-CoV-2 agents have drawn much attention from the scientific community to search for new antiviral candidates. In this study, we aimed to document the anti-SARS-CoV-2 activity of *A. paniculata* extract and andrographolide (Figure1A) for further drug development against COVID-19. Therefore, a robust anti-SARS-CoV-2 screening platform established on a legitimate model is required to facilitate this process. To serve this purpose, we optimized our antiviral assay (which was previously established upon Vero E6 cells)[30] to use Calu-3 human lung epithelial cells as the legitimate host cell for SARS-CoV-2 infection[31] and then validated the assay applicability by hydroxychloroquine and niclosamide (Figure1B and 1C, respectively), two FDA-approved drugs with anti-SAR-CoV-2 activities *in vitro*.[31−33]

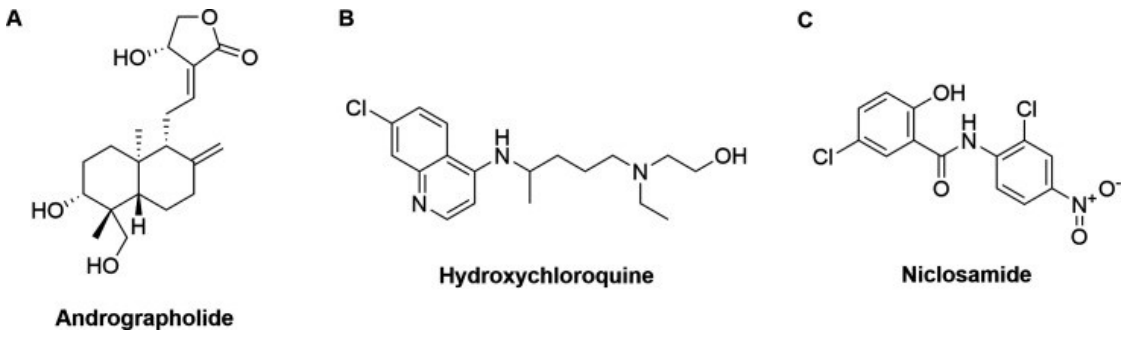

Open in a separate window

Figure 1

Chemical structures of candidate compounds for screening as anti-SARS-CoV-2 agents. Structure of the bioactive compound andrographolide extracted from *Andrographis paniculata* (A). Structures of classical FDA-approved drugs hydroxychloroquine (B) and niclosamide (C), which exhibit anti-SARS-CoV-2 activity *in vitro*.

Calu-3 cells were cultured until they reached confluence and then infected with various concentrations of SARS-CoV-2, 0.25TCID$_{50}$, 2.5TCID$_{50}$, and 25TCID$_{50}$, for 2 h. The cells were washed twice to remove the excess inoculum and further incubated in fresh culture medium for 48 h in the absence or presence of the compounds of interest. To demonstrate the degree of SARS-CoV-2 infectivity, the infected Calu-3 cells were stained by anti-SARS-CoV2 nucleoprotein rabbit monoclonal antibody, followed by goat anti-rabbit IgG Alexa Fluor 488, and the percentage of fluorescent positive cells was counted by a high-content imaging platform. The percentage of viral infectivity in Calu-3 cells at 48 h postinfection achieved approximately 1%, 18%, and 95%, upon infection at 0.25TCID$_{50}$, 2.5TCID$_{50}$, and 25TCID$_{50}$, respectively (Figure2A and B, upper panel). Since SARS-CoV-2 at 25TCID$_{50}$ was able to reach maximal infectivity, it served as the standard infectious dosage throughout all experiments. To establish the positive control, the neutralizing serum derived from COVID-19 patients with negative SARS-CoV-2 RNA was added to the infected Calu-3 cells. The high-content imaging revealed viral suppression in Calu-3 cells with a percentage of SARS-CoV-2 infectivity of 0%, 10%, 60%, and 80% at 1:100, 1:500, 1:2500, and 1:25 000 dilutions of the neutralizing serum, respectively (Figure2A and B, lower panel). In this study, anti-human IgG served as the negative control.

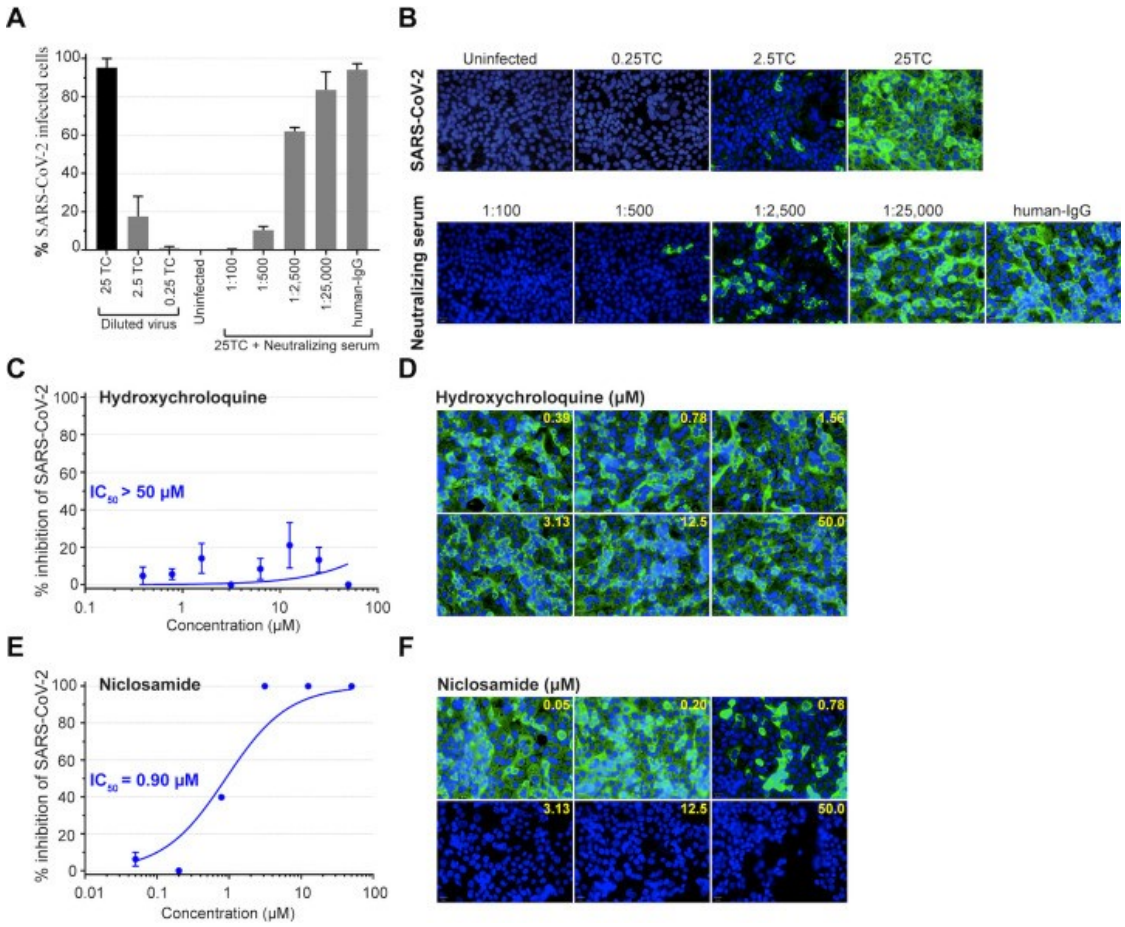

Open in a separate window

Figure 2

Optimization and validation of the anti-SARS-CoV-2 assay using human lung epithelial (Calu-3) cells. (A) The optimal dilutions of SAR-CoV-2 $TCID_{50}$, 0.25-, 2.5-, and 25-fold, were evaluated in Calu-3 cells, in which the $25TCID_{50}$ showed the maximal infectivity and was used throughout this study. FITC-labeled anti-SARS-CoV nucleoprotein mAb was used to detect the degree of SAR-CoV-2 viral replication. The positive control, neutralizing serum, demonstrated a dose-dependent effect, whereas the negative control, human IgG, had no antiviral activity. (B) Representative fluorescent images show SARS-CoV-2 infectivity at different $TCID_{50}$ (upper row) and anti-SAR-CoV-2 activity of neutralizing serum as compared to human-IgG (lower row). Fluorescent signals: green, anti-SARS-CoV NP mAb; blue, Hoechst. (C) Hydroxychloroquine exhibited no effect against SARS-CoV-2 in Calu-3 cells with $IC_{50} > 50$ μM. (D) Representative fluorescent images of the hydroxychloroquine experiment. (E) Niclosamide presented a dose-dependent anti-SARS-CoV-2 activity in Calu-3 cells with $IC_{50} = 0.90$ μM. (F) Representative fluorescent images of the niclosamide experiment.

As aforementioned, hydroxychloroquine and niclosamide[31–33] were applied to evaluate the validity of Calu-3-based anti-SARS-CoV-2 assay. Hydroxychloroquine, a classical antimalarial drug, had no inhibitory effect against SARS-CoV-2 infection in human lung epithelial cells ($IC_{50} > 50$ μM) (Figure2C and D), while niclosamide, a classical antihelminthic drug, inhibited SARS-CoV-2 infection with an IC_{50} of 0.90 μM (Figure2E and F). Of note, hydroxychloroquine can exhibit antiviral effects in Vero E6

cells[30] but not Calu-3 human lung epithelial cells.[31] These results were consistent with previous reports[31,32] and supported the validity of the Calu-3-based anti-SARS-CoV-2 assay used in this study.

Dose–Response Relationship of *A. paniculata* Extract and Andrographolide in SARS-CoV-2-Infected Human Lung Epithelial Cells

To investigate whether *A. paniculata* extract and its major component andrographolide have potential as anti-SARS-CoV-2 agents, SARS-CoV-2-infected Calu-3 cells were treated for 48 h with 4-fold dilutions of *A. paniculata* extract (0.05–50 μg/mL) or andrographolide (0.05–50 μM), respectively. The results demonstrated both *A. paniculata* extract (Figure3A and B) and andrographolide (Figure3C and D) inhibited SARS-CoV-2 replication in a dose-dependent manner.

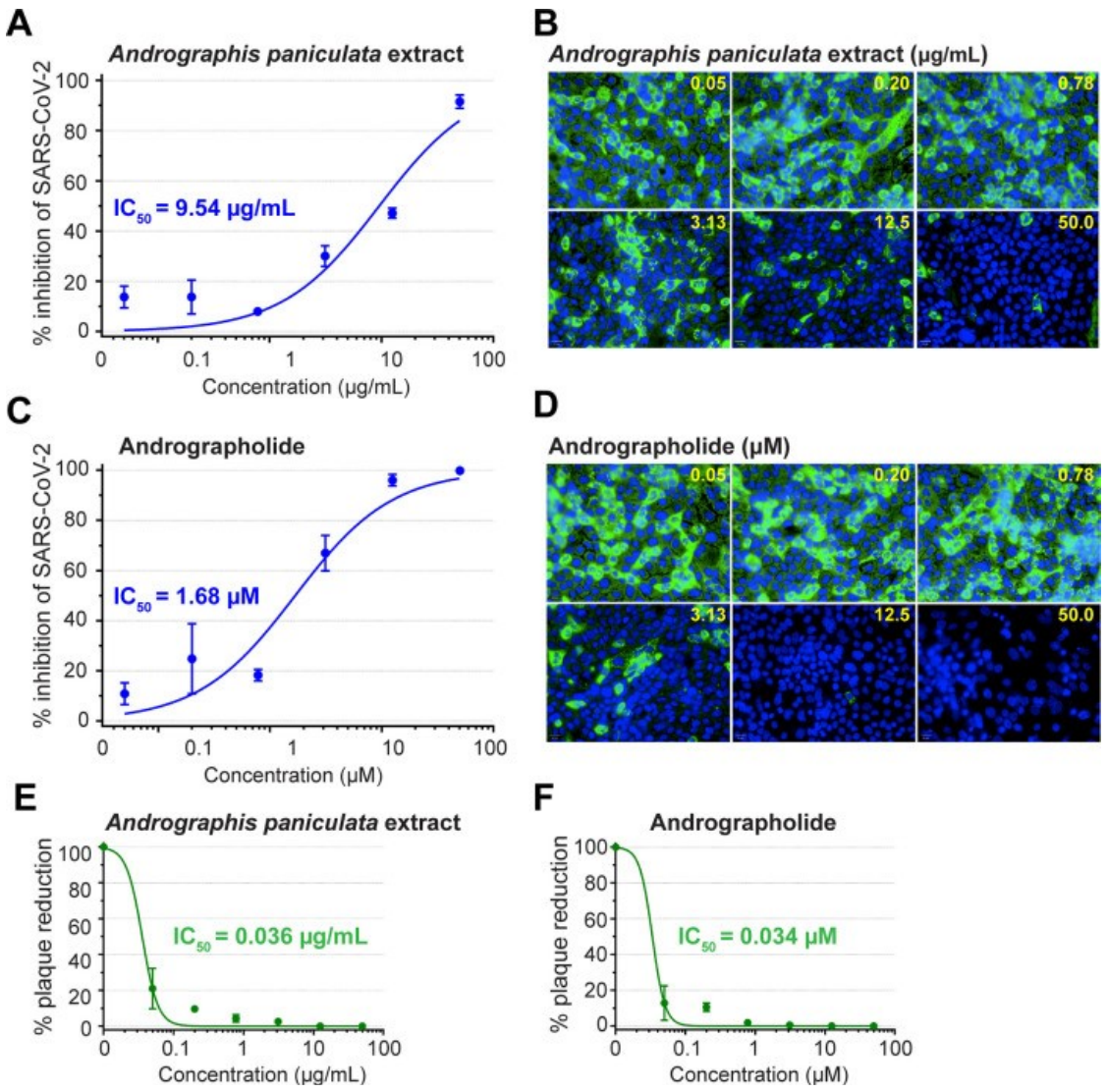

Open in a separate window

Figure 3

Anti-SARS-CoV-2 activity of *Andrographis paniculata* extract and andrographolide. SARS-CoV-2-infected Calu-3 cells (at 25TCID$_{50}$) were treated with various concentrations of *A. paniculata* extract or andrographolide for 48 h before harvesting for high-content imaging analysis. (A) *A. paniculata* extract showed the dose-dependent inhibition of SARS-CoV-2 infection. (B) Representative fluorescent images of the *A. paniculata* experiment. (C) Andrographolide, the major component of *A. paniculata* extract, exhibited potent anti-SARS-CoV-2 activity. (D) Representative fluorescent images of the andrographolide experiment. Production of infectious virions released from SARS-CoV-2-infected Calu-3 was evaluated by a plaque assay after treatment with (E) *A. paniculata* extract and (F) andrographolide. All experiments were performed in three biological replicates.

To confirm anti-SARS-CoV-2 activity of *A. paniculata* extract and andrographolide, analysis of viral output using the plaque reduction assay was performed. At 48 h postinfection in the absence or presence of compounds of interest, the culture supernatants were harvested to determine the number of

infectious virions produced from SARS-CoV-2-infected Calu-3 cells by the plaque assay. From the result, the evaluation of viral output was consistent with that of the high-content imaging study (Figure3 A–D), in which *A. paniculata* extract and andrographolide again demonstrated a dose–response relationship (Figure3E and F) with an IC_{50} of 0.036 μg/mL for *A. paniculata* and 0.034 μM for andrographolide (Figure3E and F). Similarly, evaluation of viral RNA output in the harvested supernatants by qRT-PCR also showed the reduction of the extracellular viral RNA in a dose-dependent manner following the treatment (Supplementary Figure 1). This information confirmed the significance of *A. paniculata* extract and andrographolide in suppressing SARS-CoV-2 infectivity in Calu-3 cells.

It was interesting that the IC_{50} values of *A. paniculata* extract and andrographolide varied between the high-content imaging IFA and viral output study using the plaque assay. Taking our previous study[30] into account, the IC_{50} of *A. paniculata* extract and andrographolide by measurement type and cell host is summarized in Table 1. The IC_{50} values of remdesivir[30] served as the comparators.

Table 1

IC_{50} Values of *A. paniculata* Extract, Andrographolide, and Remdesivir Evaluated by High-Content Imaging IFA and Plaque Assay in Vero E6 and Calu-3 Cells

	A. paniculata extract		andrographolide		remdesivir[a]	
cell line	IFA (IC_{50}; μg/mL)	plaque (IC_{50}; μg/mL)	IFA (IC_{50}; μM)	plaque (IC_{50}; μM)	IFA (IC_{50}; μM)	plaque (IC_{50}; μM)
Calu-3	9.54	0.036	1.68	0.034	0.043[a]	0.086[a]
Vero E6[a]	68.06[a]	2.21[a]	6.58[a]	0.28[a]	2.71[a]	2.65[a]

[a]Data from our previous study.[30]

As shown in Table 1, a consistent pattern has been detected for *A. paniculata* extract, andrographolide, and remdesivir: (i) the IC_{50} values measured from the assays using Calu-3 were lower than those of Vero E6; (ii) the IC_{50} values measured by plaque assay were lower than those of high-content imaging IFA. The deviation of drug response between two cells of different species and organs highlighted the importance of using Calu-3 human lung epithelial cells, but not Vero E6 African green monkey kidney cells, as the host cells for *in vitro* SARS-CoV-2 infection experiments.[31] The dissimilarity of IC_{50} between the IFA and the plaque assay could be explained by their different principle of SARS-CoV-2 detection. The IFA requires a specific antibody to detect the expression of SARS-CoV-2 nucleoprotein derived from complete virions and subviral particles within the host cells. On the other hand, the plaque assay measures the infectivity of complete virions released from the host cells. Compared to remdesivir, which showed similar IC_{50} values obtained from the IFA and plaque assay, treatment of Calu-3 cells with *A. paniculata* extract and andrographolide exhibited distinct IC_{50} values examined by both methods. The lower IC_{50} evaluated by the plaque assay revealed that both the extract and the compound were more potent in interfering with the production of the infectious viral progeny than inhibiting the early phase of viral genome replication and protein expression in Calu-3 cells.

Cytotoxicity Profiles of *A. paniculata* Extract and Andrographolide

One of the main concerns in medicinal plant-derived drug development is herb-induced injury of the vital organs, especially the liver. To address this issue, six human cell lines that represent five major organs, including liver (HepG2 and imHC), kidney (HK-2), intestine (Caco-2), lung (Calu-3), and brain (SH-SY5Y), were applied to evaluate the cytotoxicity profiles of *A. paniculata* extract and andrographolide by MTT assay. The results showed that the *A. paniculata* extract had no cytotoxicity to all cell lines examined, with a CC_{50} of >100 μg/mL (Figure4A). Considering the antiviral effect with an IC_{50} of 0.034 μM andrographolide (Figure3F), this diterpene lactone showed considerably low to no cytotoxic effects on the HepG2, imHC, HK-2, Caco-2, and Calu-3 cell lines, with CC_{50} values of 81.52, 44.55, 34.11, 52.30, and 58.03 μM and selectivity indexes (SI) of 2398, 1310, 1003, 1538, and 1707, respectively (Figure4B). Andrographolide-treated SH-SY5Y cells had a CC_{50} of 13.19 μM and a relatively narrower SI of 388 (Figure4B). A schematic diagram summarizing the IC_{50} and the CC_{50} values of *A. paniculata* extract and andrographolide is shown in Figure5.

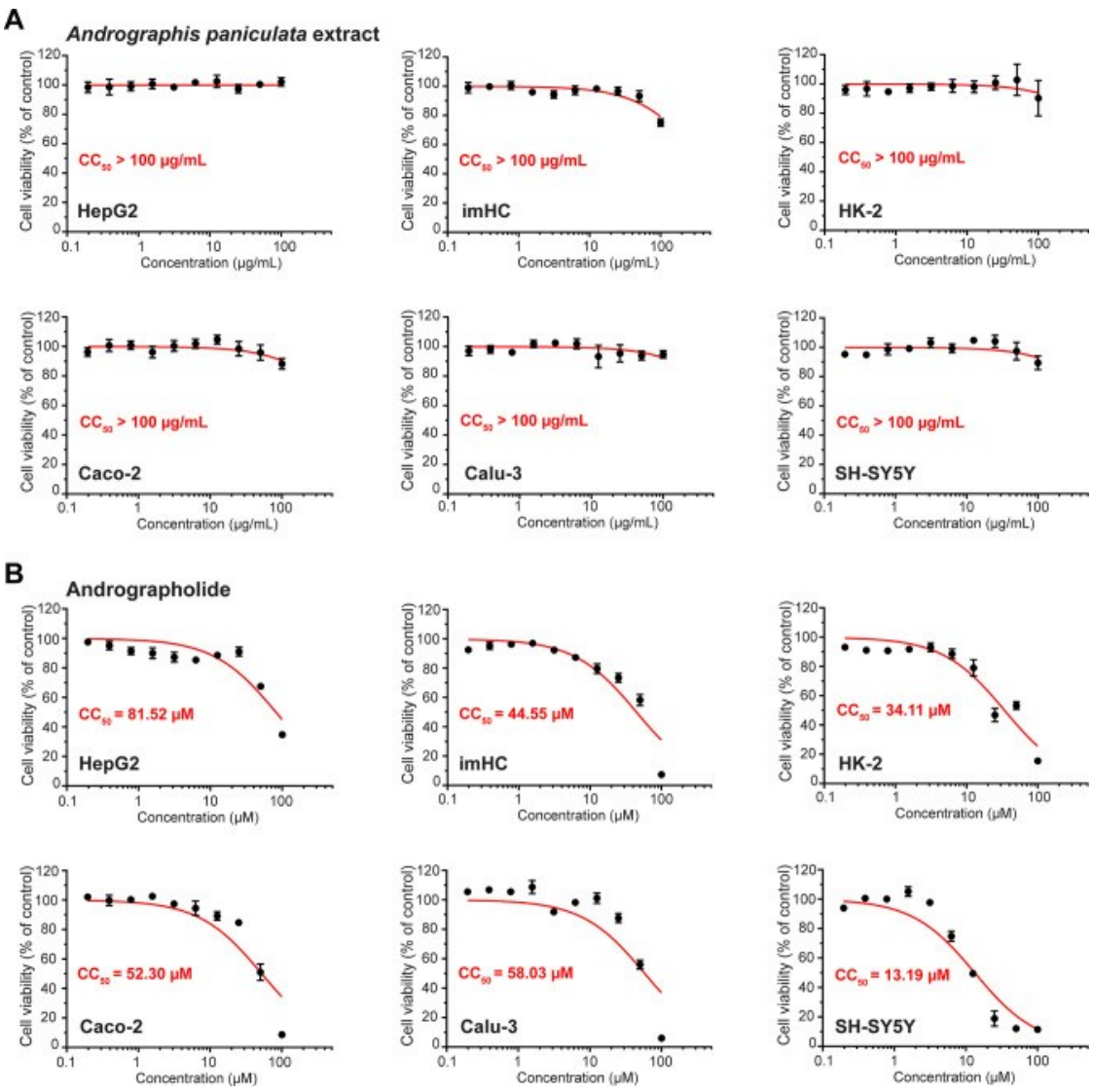

Open in a separate window

Figure 4

Cytotoxicity profiles of *A. paniculata* extract and andrographolide over six cell lines representing human major organs. After 48 h of treatment of (A) *A. paniculata* extract and (B) andrographolide in various cell lines representing the liver (HepG2, imHC), kidney (HK-2), intestine (Caco-2), lung (Calu-3), and brain (SH-SY5Y), the MTT assay was applied to evaluate the cytotoxicity effects. All experiments were performed in three biological replicates.

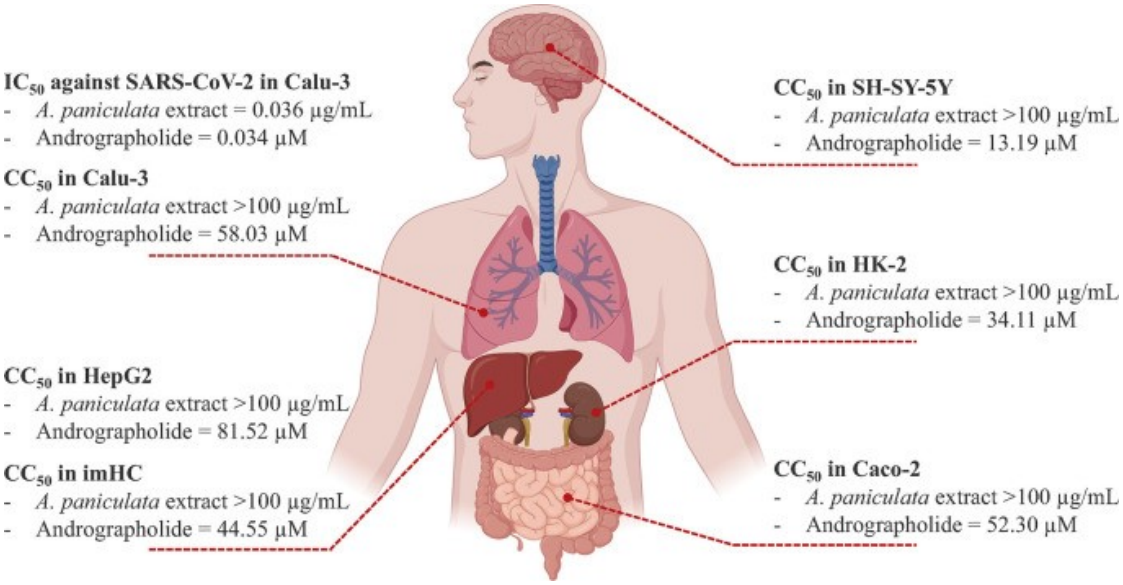

Open in a separate window

Figure 5

Schematic diagram summarizing the IC_{50} and CC_{50} of *A. paniculata* extract and andrographolide across cell line representatives of human major organs.

This finding pointed out that further development of *A. paniculata* extract and andrographolide in preclinical models of COVID-19 should pay attention to the neurologic side effects as well as the amount of andrographolide that passes through the blood–brain barrier. In this regard, the boiled-egg plot using the SwissADME program was performed for *in silico* prediction of the probability of compounds being gastrointestinal absorbable and barrier penetrating.[34,35] Based on this prediction, andrographolide is a gastrointestinal absorbable compound without an ability to pass through the blood–brain barrier (Supplementary Figure 2). The SwissADME prediction also reveals that andrographolide is a P-glycoprotein (P-gp) substrate,[36] suggesting that andrographolide would be "pumped out" from central nervous system (CNS) tissues and may not possess significant neurotoxicity if used in further studies.

Potential Clinical Applications of *A. paniculata* Extract and Andrographolide

A. paniculata has been classified as an essential plant for traditional medicine in various Asian countries for centuries.[37] In Thailand, the Ministry of Public Health has registered this plant, so-called Fah Talai Jone, on The National List of Essential Drugs A.D. 1999 (List of Herbal Medicinal Products).[38] *A. paniculata* extract has long been available in Thailand's markets as herbal nutraceuticals in several recipes and brands, which the general population can access and use to treat diarrhea, fever, the common cold, and viral infection. It is postulated that beneficial effects of *A. paniculata* extract largely depend on its major component, andrographolide, the bicyclic diterpene lactone with multifunctionalities including anticancer, antioxidant, anti-inflammatory, immunomodulatory, cardiovascular protection and hepatoprotection, antimicrobial, and antiprotozoal effects.[37,39–42]

Andrographolide is also well known for its broad-spectrum antiviral properties.[24] Studies showed

andrographolide is effective against influenza A,[43] hepatitis C virus,[44] Chikungunya virus,[40] HIV,[45] hepatitis B virus,[46] Herpes simplex virus 1,[47] Epstein–Barr virus,[48] and human papillomavirus.[49] This study showed that both *A. paniculata* extract and its active component andrographolide had a potent inhibitory effect against SARS-CoV-2. This finding opens the possibility to develop *A. paniculata* extract and andrographolide in the context of COVID-19 treatment. In comparison to our previous study,[30] *A. paniculata* extract and andrographolide exhibited the equivalent IC_{50} against SARS-CoV-2 infection to remdesivir[30] (Table 1). This is an additional rationale to support *A. paniculata* extract and especially andrographolide for further antiviral development.

Previous studies suggested andrographolide targeted nonstructural proteins of SARS-CoV-2 as the mechanism of action. An enzyme-based assay and *in silico* modeling prediction showed andrographolide could inhibit the main protease (M^{pro}) activities of SARS-CoV-2 with an IC_{50} of 15 μM.[26,29] When compared to our finding, the IC_{50} from the M^{pro} enzyme-based assay was 10 times higher, implying that andrographolide probably functions through multiple targets as previously predicted by *in silico* models.[25−28] It has been proposed that andrographolide is involved in multiple steps of the viral life cycle including viral entry, genetic material replication, and protein synthesis and inhibits the expression or function of the mature proteins.[24] Maurya et al.[50] showed that andrographolide has significant binding affinity toward the spike glycoprotein of both SARS-CoV-2 and ACE2 receptors and could be developed as a prophylactic agent for limiting viral entry into the host cells.

In this study, we applied two assays to evaluate the anti-SARS-CoV-2 activity in Calu-3 cells. Since both IFA and plaque assays investigate the distinct steps in the SARS-CoV-2 life cycle (the expression of viral protein *vs* the production of infectious progenies), interpretation of IC_{50} values of the compound obtained from such assays could be made differently. This depends on the potency of the extract or compound in perturbing a specific step of the SARS-CoV-2 life cycle, either the viral protein expression or the particle release. Therefore, the IC_{50} value obtained from IFA could be interpreted as the half-maximal concentration of the compound able to inhibit SARS-CoV-2 NP expression. On the other hand, the IC_{50} value from the plaque assay could be indicated as the half-maximal concentration of the compound able to inhibit infectious virion production. From our data, the IC_{50} values measured by the plaque assay were lower than those of the high-content imaging IFA. This can be interpreted as both *A. paniculata* extract and andrographolide are more potent in interfering at the late phases of the viral life cycle in Calu-3 cells than those of the early steps of viral genome replication and protein expression. The late phases of the SARS-CoV-2 life cycle include viral assembly and maturation, transportation along the secretory pathway, or particle release. Also, we performed pre-entry treatment of andrographolide in Vero E6 cells (Supplementary Figure 3), in which the compound was added into the cells together with the 25TCID50 of SARS-CoV-2 during the viral adsorption step. Then the inoculum was removed, and the cells were washed before adding fresh medium without the compound into the cells. In this pre-entry treatment, the IC_{50} of andrographolide evaluated by IFA was 19.03 μM, compared with the IC_{50} value of 6.58 μM in the post-treatment condition.[51] This suggested that the compound might target the postentry event or the late phase of the viral life cycle. Since andrographolide exerted a stronger anti-SARS-CoV-2 effect than the extract, this finding highlighted this compound as a potential monotherapy, even though the combinational regimens with other compounds that interfere with the early phase of the viral life cycle, such as remdesivir, should be prioritized to increase the efficacy and minimize the side effects/toxicities.

This study was associated with several limitations. Although our findings support andrographolide as a promising candidate for further anti-SARS-CoV-2 development, the low bioavailability of andrographolide might pose a limitation for clinical applications.[52,53] Several strategies have been

developed to improve andrographolide solubility and bioavailability, i.e., forming complexes with hydroxypropyl-β-cyclodextrin (HP-β-CD),[54] solid dispersion using a spray-drying technique,[55] and loading into the nanoemulsion.[56] Also, it should be noted that this study was conducted using an *in vitro* cellular model. The safety and efficacy of andrographolide should be further investigated in preclinical animal models and clinical studies.

In conclusion, this study demonstrated anti-SARS-CoV-2 activity of *A. paniculata* and andrographolide using a Calu-3-based anti-SARS-CoV-2 assay. Potent anti-SAR-CoV-2 activities, together with the favorable cytotoxicity profiles, support further development of *A. paniculata* extract and especially andrographolide as a monotherapy or in combination with other effective drugs against SARS-CoV-2 infection.

Experimental Section

Cell Culture

African green monkey (*Cercopithecus aethiops*) kidney epithelial cells (Vero cells) (ATCC CCL-81), a Vero cell derivative (Vero E6 cells) (ATCC CRL-1586), a human liver cancer cell line (HepG2) (ATCC HB-8065), a human colon cancer cell line (Caco-2) (ATCC HTB-37), a human airway epithelial cell line (Calu-3) (ATCC HTB-55), a human neuroblastoma cell line (SH-SY5Y) (ATCC CRL-2266), and human normal kidney (HK-2) (ATCC CRL-2190) cells were obtained from American Type Culture Collection (ATCC, Manassas, VA, USA). An immortalized hepatocyte-like cell line (imHC) was established in-house as previously described,[57] and its hepatic phenotypes were characterized previously.[58,59] Vero cells were cultured in minimum essential medium (MEM) (Gibco, Detroit, MI, USA). Vero E6 and Caco-2 cells were cultured in Dulbecco's modified Eagle's medium (DMEM) (Gibco). HepG2, imHC, Calu-3, and SH-SY5Y cells were cultured in DMEM:nutrient mixture F-12 (Gibco). HK-2 cells were cultured in Dulbecco's low glucose modified Eagle's medium (DMEM low glucose) (HyClone, Logan, UT, USA). The culture media was supplemented with 10% fetal bovine serum (FBS) (Thermo Scientific Fisher, Waltham, MA, USA) and 100 μg/mL penicillin/streptomycin (Invitrogen, Carlsbad, CA, USA) and 1% GlutaMAX (Gibco). Cells were incubated at 37 °C in a humidified incubator with 5% CO_2.

Preparation of SARS-CoV-2 Virus

SARS-CoV-2 virus was isolated from nasopharyngeal swabs of a confirmed COVID-19 patient in Thailand (SARS-CoV-2/01/human/Jan2020/Thailand). The virus was propagated in Vero E6 cells as previously described[30] and stored at −80 °C. Viral titration as $TCID_{50}$ titer/mL was performed in a 96-well plate. In brief, the virus stock was titrated in quadruplicate in 96-well plates on Vero E6 cells in serial dilution to obtain 50% tissue culture infectious dose ($TCID_{50}$) using the Reed–Muench method.[60] All the experiments with live SARS-CoV-2 viruses were performed at a certified biosafety level 3 facility at Department of Microbiology, Faculty of Science, Mahidol University.

Preparation of *Andrographis paniculata* Extract and Andrographolide

Plant material in this study was common herbs in Thailand, and it was listed in Thai Herbal Pharmacopoeia 2019 (https://bdn.go.th/th/sDetail/10/34/). The plant was identified, authenticated by Chao Phya Abhaibhubejhr Hospital, Prachin Buri, Thailand, and deposited at the herbarium unit. The powder of *A. paniculata* was weighed and soaked in 95% ethanol in a ratio of 1:4. After 24 h, the liquid fraction was separated using a thin straining cloth, then filtered through filter paper by a vacuum pump. The extract obtained was concentrated using a rotary evaporator at a temperature of 45 °C and then concentrated in a water bath at 70 °C until it became a concentrated solution. The crude extract was stored at 4 °C and protected from light until use.[61] The andrographolide concentration in the crude

extract was measured by the HPLC method following the Thai Herbal Pharmacopoeia 2019 protocol. The andrographolide content in the crude extract was 7.9% (w/w).[62] The analytical standard andrographolide was used as a reference (Sigma, St. Louis, MO, USA).

In Vitro Antiviral Assay

Calu-3 cells were seeded at 1×10^4 cells per well in a 96-well black plate (Corning, NY, USA) and incubated for 24 h at 37 °C in a 5% CO_2 atmosphere. Then, culture medium was discarded and washed once with phosphate-buffered saline (PBS). Cells were infected with SARS-CoV-2 at 25$TCID_{50}$ for 2 h at 37 °C. After viral adsorption, the cells were washed twice with PBS to remove the excess inoculum, and the fresh culture medium (DMEM/F12 supplemented with 10% FBS and 100 µg/mL penicillin/streptomycin) was added. Each concentration of drugs, crude extract, or active compound was inoculated into the culture medium. Infected cells were then maintained at 37 °C in a 5% CO_2 incubator for 48 h. Positive convalescent serum (heat-inactivated at 56 °C for 30 min) of a COVID-19 patient and anti-human IgG (Santa Cruz Biotechnology, Dallas, TX, USA) were used for viral inhibition as positive control and negative control, respectively. The experiment was performed in triplicate.

High-Content Imaging for SARS-CoV Nucleoprotein Detection

The cells in the 96-well plate were fixed and permeabilized with 50% (v/v) acetone in methanol on ice for 20 min. The fixed cells were washed once with PBS with 0.5% Tween detergent (PBST) and blocked with 2% (w/v) BSA in PBST for 1 h at room temperature. Next, the cells were incubated with a 1:500 dilution ratio of primary antibody specific for SARS-CoV nucleoprotein[56] (rabbit mAb) (Sino Biological Inc. China), which cross-reacted with the NP protein of SARS-CoV-2 as well, for 1 h at 37 °C. After incubation, cells were washed with PBST three times. Then, the goat anti-rabbit IgG Alexa Fluor 488 (Thermo Fisher Scientific, Waltham, MA, USA) was used as the secondary antibody at 1:500 dilution. Hoechst dye (Thermo Fisher Scientific) was applied for nuclei staining. The fluorescent signal was detected and analyzed by the Operetta high-content imaging system (PerkinElmer, Waltham, MA, USA) as previously described.[30] Percentage of infected cells in each well was automatically obtained from 13 fields per well using Harmony software (PerkinElmer). Data were normalized to the infected control, and the IC_{50} value was calculated by GraphPad Prism 7.

Plaque Assay

The viral output in culture supernatants obtained from SARS-CoV-2-infected Calu-3 cells was determined by plaque assay by using a Vero cell monolayer. In brief, Vero cells were seeded into a six-well plate 24 h prior to infection. A serial dilution of the virus-containing supernatants was prepared for inoculation into the Vero cell monolayer. The cells were incubated for viral adsorption for 1 h in a 37 °C incubator and then overlaid with 3 mL/well of MEM medium supplemented with 5% FBS and 1% agarose. The culture was incubated at 37 °C in 5% CO_2 for 3 days. Thereafter, plaque phenotypes were visualized by staining with 0.33% Neutral Red solution (Sigma-Aldrich) for 5 h. Plaque numbers were counted as plaque-forming units per milliliter and reported as the percentage of plaque reduction in comparison to supernatant obtained from the infected Calu-3 cells without any treatment.

Cell Cytotoxicity Assay

All human cell lines were plated in 96-well plates at 5×10^4 cells/well and treated with various concentrations of *A. paniculata* extract (0–100 µg/mL) and andrographolide (0–100 µM) for 48 h. Cell viability was examined by an MTT colorimetric assay. In brief, the medium was replaced with MTT [3-(4,5-dimethylthiazol-2-yl)-2,5-diphenyltetrazolium bromide] (Sigma-Aldrich) at a final concentration

of 0.5 mg/mL and incubated for 4 h at 37 °C in a humidified incubator with 5% CO_2. The rest of the MTT solution was removed, and formazan crystals were then dissolved with DMSO (Merck, Schuchardt, Darmstadt, Germany). Absorbance was measured at a wavelength of 570 nm by an EnVision multilabel reader (PerkinElmer). Data were normalized to the solvent control, and then CC_{50} values were calculated using GraphPad Prism 7.

Acknowledgments

We thank the Department of Disease Control, Ministry of Public Health Thailand, for providing the clinical specimens for viral isolation. This study was supported by the Ramathibodi Research Cluster Grant (CF63010), Faculty of Medicine Ramathibodi Hospital, and Faculty of Science, Mahidol University, Thailand. K.S. was financially supported by the Office of National Higher Education Science Research and Innovation Policy Council through Program Management Unit for Competitiveness (C10F630093). S.K. was supported by The Royal Golden Jubilee (RGJ) Ph.D. Program Scholarship from the Thailand Research Fund (Grant No. PHD/0009/2558; RGJ 18). So.C. was financially supported by the Faculty Staff Development Program of the Faculty of Medicine Ramathibodi Hospital and the Office of National Higher Education Science Research and Innovation Policy Council of Thailand (NXPO; PMU-B). S.H. was supported by the Ramathibodi Foundation. S.B. was supported by the Thailand Center of Excellence for Life Sciences (TCELS) Grant (TC-A15/63). A.T. was supported by the Chaophaya Abhaibhubejhr Hospital Foundation. This research project is supported by Mahidol University, Thailand.

Notes

Supporting Information Available

The Supporting Information is available free of charge at https://pubs.acs.org/doi/10.1021/acs.jnatprod.0c01324.

Additional figures and Supplementary Method 1 (PDF)

Author Contributions

S.B., A.T., and S.H. initiated the conception. A.S., P.Kh., So.C., S.B., A.T., and S.H. developed the design. K.S., Y.P., P.T., P.Ka., S.M., Si.C., J.C., S.K., K.J., and W.W. performed experiments. All authors analyzed and interpreted the data. K.S., A.S., Y.P., P.K., Si.C., and So.C. prepared figures and tables. K.S. and A.S. wrote the first draft of the manuscript. Y.P., P.T., P.Ka., S.M., Si.C., P.W., S.P., P.Kh., So.C., S.B., A.T., and S.H. revised the manuscript. S.B. and A.T. finalized the manuscript. S.H. contributed to the overall research strategy. All authors read and approved the final version of the manuscript.

Author Contributions

[#] K.S. and A.S. contributed equally to this work.

Notes

The authors declare no competing financial interest.

Supplementary Material

np0c01324_si_005.pdf (301K, pdf)

References

1. Huang J. T.; Ran R. X.; Lv Z. H.; Feng L. N.; Ran C. Y.; Tong Y. Q.; Li D.; Su H. W.; Zhu C. L.; Qiu S. L.; Yang J.; Xiao M. Y.; Liu M. J.; Yang Y. T.; Liu S. M.; Li Y.. Chronological Changes of Viral Shedding in Adult Inpatients with COVID-19 in Wuhan, China. *Clin. Infect. Dis.* 2020.712158.10.1093/cid/ciaa631 [PMC free article] [PubMed] [CrossRef] [Google Scholar]
2. Chan J. F. W.; Lau S. K. P.; To K. K. W.; Cheng V. C. C.; Woo P. C. Y.; Yuen K.-Y.. Middle East Respiratory Syndrome Coronavirus: Another Zoonotic Betacoronavirus Causing SARS-Like Disease.*Clin. Microbiol. Rev.* 2015, 28 ((2),), 465–522.10.1128/CMR.00102-14 [PMC free article] [PubMed] [CrossRef] [Google Scholar]
3. Cheng V. C.; Lau S. K.; Woo P. C.; Yuen K. Y. Severe acute respiratory syndrome coronavirus as an agent of emerging and reemerging infection. *Clin. Microbiol. Rev.* 2007, 20 (4), 660–94. 10.1128/CMR.00023-07. [PMC free article] [PubMed] [CrossRef] [Google Scholar]
4. Zhu N.; Zhang D.; Wang W.; Li X.; Yang B.; Song J.; Zhao X.; Huang B.; Shi W.; Lu R.; Niu P.; Zhan F.; Ma X.; Wang D.; Xu W.; Wu G.; Gao G. F.; Tan W.; China Novel Coronavirus I.; Research T. A Novel Coronavirus from Patients with Pneumonia in China, 2019. *N. Engl. J. Med.* 2020, 382 (8), 727–733. 10.1056/NEJMoa2001017. [PMC free article] [PubMed] [CrossRef] [Google Scholar]
5. Gorbalenya A. E.; Baker S. C.; Baric R. S.; de Groot R. J.; Drosten C.; Gulyaeva A. A.; Haagmans B. L.; Lauber C.; Leontovich A. M.; Neuman B. W.; Penzar D.; Perlman S.; Poon L. L. M.; Samborskiy D. V.; Sidorov I. A.; Sola I.; Ziebuhr J. Coronaviridae Study Group of the International Committee on Taxonomy of, V. The species Severe acute respiratory syndrome-related coronavirus: classifying 2019-nCoV and naming it SARS-CoV-2. *Nat. Microbiol.* 2020, 5 (4), 536–544. 10.1038/s41564-020-0695-z. [PMC free article] [PubMed] [CrossRef] [Google Scholar]
6. Chan J. F.-W.; Yuan S.; Kok K.-H.; To K. K.-W.; Chu H.; Yang J.; Xing F.; Liu J.; Yip C. C.-Y.; Poon R. W.-S.; Tsoi H.-W.; Lo S. K.-F.; Chan K.-H.; Poon V. K.-M.; Chan W.-M.; Ip J. D.; Cai J.-P.; Cheng V. C.-C.; Chen H.; Hui C. K.-M.; Yuen K.-Y. A familial cluster of pneumonia associated with the 2019 novel coronavirus indicating person-to-person transmission: a study of a family cluster. *Lancet* 2020, 395 (10223), 514–523. 10.1016/S0140-6736(20)30154-9. [PMC free article] [PubMed] [CrossRef] [Google Scholar]
7. Jiehao C.; Jin X.; Daojiong L.; Zhi Y.; Lei X.; Zhenghai Q.; Yuehua Z.; Hua Z.; Ran J.; Pengcheng L.; Xiangshi W.; Yanling G.; Aimei X.; He T.; Hailing C.; Chuning W.; Jingjing L.; Jianshe W.; Mei Z. A Case Series of Children With 2019 Novel Coronavirus Infection: Clinical and Epidemiological Features. *Clin. Infect. Dis.* 2020, 71 (6), 1547–1551. 10.1093/cid/ciaa198. [PMC free article] [PubMed] [CrossRef] [Google Scholar]
8. Verity R.; Okell L. C.; Dorigatti I.; Winskill P.; Whittaker C.; Imai N.; Cuomo-Dannenburg G.; Thompson H.; Walker P. G. T.; Fu H.; Dighe A.; Griffin J. T.; Baguelin M.; Bhatia S.; Boonyasiri A.; Cori A.; Cucunuba Z.; FitzJohn R.; Gaythorpe K.; Green W.; Hamlet A.; Hinsley W.; Laydon D.; Nedjati-Gilani G.; Riley S.; van Elsland S.; Volz E.; Wang H.; Wang Y.; Xi X.; Donnelly C. A.; Ghani A. C.; Ferguson N. M. Estimates of the severity of coronavirus disease 2019: a model-based analysis. *Lancet Infect. Dis.* 2020, 20 (6), 669–677. 10.1016/S1473-3099(20)30243-7.

[PMC free article] [PubMed] [CrossRef] [Google Scholar]
9. Guan W. J.; Ni Z. Y.; Hu Y.; Liang W. H.; Ou C. Q.; He J. X.; Liu L.; Shan H.; Lei C. L.; Hui D. S. C.; Du B.; Li L. J.; Zeng G.; Yuen K. Y.; Chen R. C.; Tang C. L.; Wang T.; Chen P. Y.; Xiang J.; Li S. Y.; Wang J. L.; Liang Z. J.; Peng Y. X.; Wei L.; Liu Y.; Hu Y. H.; Peng P.; Wang J. M.; Liu J. Y.; Chen Z.; Li G.; Zheng Z. J.; Qiu S. Q.; Luo J.; Ye C. J.; Zhu S. Y.; Zhong N. S. China Medical Treatment Expert Group for, C. Clinical Characteristics of Coronavirus Disease 2019 in China. *N. Engl. J. Med.* 2020, 382 (18), 1708–1720. 10.1056/NEJMoa2002032. [PMC free article] [PubMed] [CrossRef] [Google Scholar]
10. Huang C.; Wang Y.; Li X.; Ren L.; Zhao J.; Hu Y.; Zhang L.; Fan G.; Xu J.; Gu X.; Cheng Z.; Yu T.; Xia J.; Wei Y.; Wu W.; Xie X.; Yin W.; Li H.; Liu M.; Xiao Y.; Gao H.; Guo L.; Xie J.; Wang G.; Jiang R.; Gao Z.; Jin Q.; Wang J.; Cao B. Clinical features of patients infected with 2019 novel coronavirus in Wuhan, China. *Lancet* 2020, 395 (10223), 497–506. 10.1016/S0140-6736(20)30183-5. [PMC free article] [PubMed] [CrossRef] [Google Scholar]
11. Jeon S.; Ko M.; Lee J.; Choi I.; Byun S. Y.; Park S.; Shum D.; Kim S. Identification of Antiviral Drug Candidates against SARS-CoV-2 from FDA-Approved Drugs. *Antimicrob. Agents Chemother.* 2020, 64 (7), e0081910.1128/AAC.00819-20. [PMC free article] [PubMed] [CrossRef] [Google Scholar]
12. Riva L.; Yuan S.; Yin X.; Martin-Sancho L.; Matsunaga N.; Pache L.; Burgstaller-Muehlbacher S.; De Jesus P. D.; Teriete P.; Hull M. V.; Chang M. W.; Chan J. F.; Cao J.; Poon V. K.; Herbert K. M.; Cheng K.; Nguyen T. H.; Rubanov A.; Pu Y.; Nguyen C.; Choi A.; Rathnasinghe R.; Schotsaert M.; Miorin L.; Dejosez M.; Zwaka T. P.; Sit K. Y.; Martinez-Sobrido L.; Liu W. C.; White K. M.; Chapman M. E.; Lendy E. K.; Glynne R. J.; Albrecht R.; Ruppin E.; Mesecar A. D.; Johnson J. R.; Benner C.; Sun R.; Schultz P. G.; Su A. I.; Garcia-Sastre A.; Chatterjee A. K.; Yuen K. Y.; Chanda S. K. Discovery of SARS-CoV-2 antiviral drugs through large-scale compound repurposing. *Nature* 2020, 586 (7827), 113–119. 10.1038/s41586-020-2577-1. [PMC free article] [PubMed] [CrossRef] [Google Scholar]
13. Shyr Z. A.; Gorshkov K.; Chen C. Z.; Zheng W. Drug Discovery Strategies for SARS-CoV-2. *J. Pharmacol. Exp. Ther.* 2020, 375 (1), 127–138. 10.1124/jpet.120.000123. [PMC free article] [PubMed] [CrossRef] [Google Scholar]
14. Choy K. T.; Wong A. Y.; Kaewpreedee P.; Sia S. F.; Chen D.; Hui K. P. Y.; Chu D. K. W.; Chan M. C. W.; Cheung P. P.; Huang X.; Peiris M.; Yen H. L. Remdesivir, lopinavir, emetine, and homoharringtonine inhibit SARS-CoV-2 replication in vitro. *Antiviral Res.* 2020, 178, 104786.10.1016/j.antiviral.2020.104786. [PMC free article] [PubMed] [CrossRef] [Google Scholar]
15. Spinner C. D.; Gottlieb R. L.; Criner G. J.; Arribas Lopez J. R.; Cattelan A. M.; Soriano Viladomiu A.; Ogbuagu O.; Malhotra P.; Mullane K. M.; Castagna A.; Chai L. Y. A.; Roestenberg M.; Tsang O. T. Y.; Bernasconi E.; Le Turnier P.; Chang S. C.; SenGupta D.; Hyland R. H.; Osinusi A. O.; Cao H.; Blair C.; Wang H.; Gaggar A.; Brainard D. M.; McPhail M. J.; Bhagani S.; Ahn M. Y.; Sanyal A. J.; Huhn G.; Marty F. M.; Investigators G.-U. Effect of Remdesivir vs Standard Care on Clinical Status at 11 Days in Patients With Moderate COVID-19: A Randomized Clinical Trial. *JAMA* 2020, 324 (11), 1048–1057. 10.1001/jama.2020.16349. [PMC free article] [PubMed] [CrossRef] [Google Scholar]
16. Beigel J. H.; Tomashek K. M.; Dodd L. E.; Mehta A. K.; Zingman B. S.; Kalil A. C.; Hohmann E.; Chu H. Y.; Luetkemeyer A.; Kline S.; Lopez de Castilla D.; Finberg R. W.; Dierberg K.; Tapson V.; Hsieh L.; Patterson T. F.; Paredes R.; Sweeney D. A.; Short W. R.; Touloumi G.; Lye D. C.; Ohmagari N.; Oh M. D.; Ruiz-Palacios G. M.; Benfield T.; Fatkenheuer G.; Kortepeter M. G.; Atmar R. L.; Creech C. B.; Lundgren J.; Babiker A. G.; Pett S.; Neaton J. D.; Burgess T. H.; Bonnett T.; Green M.; Makowski M.; Osinusi A.; Nayak S.; Lane H. C.; Members A.-S. G.

Remdesivir for the Treatment of Covid-19 - Final Report. *N. Engl. J. Med.* 2020, 383 (19), 1813–1826. 10.1056/NEJMoa2007764. [PMC free article] [PubMed] [CrossRef] [Google Scholar]

17. Dyer O. Covid-19: Remdesivir has little or no impact on survival, WHO trial shows. *BMJ.* 2020, 371, m405710.1136/bmj.m4057. [PubMed] [CrossRef] [Google Scholar]
18. Newman D. J.; Cragg G. M. Natural Products as Sources of New Drugs from 1981 to 2014. *J. Nat. Prod.* 2016, 79 (3), 629–661. 10.1021/acs.jnatprod.5b01055. [PubMed] [CrossRef] [Google Scholar]
19. Siddiqui A. J.; Danciu C.; Ashraf S. A.; Moin A.; Singh R.; Alreshidi M.; Patel M.; Jahan S.; Kumar S.; Alkhinjar M. I. M.; Badraoui R.; Snoussi M.; Adnan M. Plants-Derived Biomolecules as Potent Antiviral Phytomedicines: New Insights on Ethnobotanical Evidences against Coronaviruses. *Plants* 2020, 9 (9), 1244.10.3390/plants9091244. [PMC free article] [PubMed] [CrossRef] [Google Scholar]
20. Khare P.; Sahu U.; Pandey S. C.; Samant M. Current approaches for target-specific drug discovery using natural compounds against SARS-CoV-2 infection. *Virus Res.* 2020, 290, 198169.10.1016/j.virusres.2020.198169. [PMC free article] [PubMed] [CrossRef] [Google Scholar]
21. Pholphana N.; Rangkadilok N.; Saehun J.; Ritruechai S.; Satayavivad J. Changes in the contents of four active diterpenoids at different growth stages in Andrographis paniculata (Burm.f.) Nees (Chuanxinlian). *Chin. Med.* 2013, 8 (1), 2.10.1186/1749-8546-8-2. [PMC free article] [PubMed] [CrossRef] [Google Scholar]
22. Hossain M. S.; Urbi Z.; Sule A.; Hafizur Rahman K. M. Andrographis paniculata (Burm. f.) Wall. ex Nees: a review of ethnobotany, phytochemistry, and pharmacology. *Sci. World J.* 2014, 2014, 274905. [PMC free article] [PubMed] [Google Scholar]
23. Koteswara Rao Y.; Vimalamma G.; Rao C. V.; Tzeng Y. M. Flavonoids and andrographolides from Andrographis paniculata. *Phytochemistry* 2004, 65 (16), 2317–21. 10.1016/j.phytochem.2004.05.008. [PubMed] [CrossRef] [Google Scholar]
24. Gupta S.; Mishra K. P.; Ganju L. Broad-spectrum antiviral properties of andrographolide. *Arch. Virol.* 2017, 162 (3), 611–623. 10.1007/s00705-016-3166-3. [PubMed] [CrossRef] [Google Scholar]
25. Alagu Lakshmi S.; Shafreen R. M. B.; Priya A.; Shunmugiah K. P. Ethnomedicines of Indian origin for combating COVID-19 infection by hampering the viral replication: using structure-based drug discovery approach. *J. Biomol. Struct. Dyn.* 2020, 1–16. [PMC free article] [PubMed] [Google Scholar]
26. Enmozhi S. K.; Raja K.; Sebastine I.; Joseph J. Andrographolide as a potential inhibitor of SARS-CoV-2 main protease: an in silico approach. *J. Biomol. Struct. Dyn.* 2020, 1–7. [PMC free article] [PubMed] [Google Scholar]
27. Linda Laksmiani N. P.; Febryana Larasanty L. P.; Gde Jaya Santika A. A.; Andika Prayoga P. A.; Intan Kharisma Dewi A. A.; Ayu Kristiara Dewi N. P. Active Compounds Activity from the Medicinal Plants Against SARS-CoV-2 using in Silico Assay. *Biomed. Pharmacol. J.* 2020, 13 (02), 873–881. 10.13005/bpj/1953. [CrossRef] [Google Scholar]
28. Murugan N. A.; Pandian C. J.; Jeyakanthan J. Computational investigation on Andrographis paniculata phytochemicals to evaluate their potency against SARS-CoV-2 in comparison to known antiviral compounds in drug trials. *J. Biomol. Struct. Dyn.* 2020, 1–12. [PubMed] [Google Scholar]
29. Shi T. H.; Huang Y. L.; Chen C. C.; Pi W. C.; Hsu Y. L.; Lo L. C.; Chen W. Y.; Fu S. L.; Lin C. H.. Andrographolide and its fluorescent derivative inhibit the main proteases of 2019-nCoV and SARS-CoV through covalent linkage. *Biochem. Biophys. Res. Commun.* 2020, 533,

467.10.1016/j.bbrc.2020.08.086. [PMC free article] [PubMed] [CrossRef] [Google Scholar]
30. Kanjanasirirat P.; Suksatu A.; Manopwisedjaroen S.; Munyoo B.; Tuchinda P.; Jearawuttanakul K.; Seemakhan S.; Charoensutthivarakul S.; Wongtrakoongate P.; Rangkasenee N.; Pitiporn S.; Waranuch N.; Chabang N.; Khemawoot P.; Sa-Ngiamsuntorn K.; Pewkliang Y.; Thongsri P.; Chutipongtanate S.; Hongeng S.; Borwornpinyo S.; Thitithanyanont A. High-content screening of Thai medicinal plants reveals Boesenbergia rotunda extract and its component Panduratin A as anti-SARS-CoV-2 agents. *Sci. Rep.* 2020, 10 (1), 19963.10.1038/s41598-020-77003-3. [PMC free article] [PubMed] [CrossRef] [Google Scholar]
31. Hoffmann M.; Mosbauer K.; Hofmann-Winkler H.; Kaul A.; Kleine-Weber H.; Kruger N.; Gassen N. C.; Muller M. A.; Drosten C.; Pohlmann S. Chloroquine does not inhibit infection of human lung cells with SARS-CoV-2. *Nature* 2020, 585 (7826), 588–590. 10.1038/s41586-020-2575-3. [PubMed] [CrossRef] [Google Scholar]
32. Jeon S.; Ko M.; Lee J.; Choi I.; Byun S. Y.; Park S.; Shum D.; Kim S., Identification of Antiviral Drug Candidates against SARS-CoV-2 from FDA-Approved Drugs. *Antimicrob. Agents Chemother.* 2020, 64 ((7),). [PMC free article] [PubMed] [Google Scholar]
33. Pindiprolu S.; Pindiprolu S. H. Plausible mechanisms of Niclosamide as an antiviral agent against COVID-19. *Med. Hypotheses* 2020, 140, 109765.10.1016/j.mehy.2020.109765. [PMC free article] [PubMed] [CrossRef] [Google Scholar]
34. Daina A.; Michielin O.; Zoete V. SwissADME: a free web tool to evaluate pharmacokinetics, drug-likeness and medicinal chemistry friendliness of small molecules. *Sci. Rep.* 2017, 7 (1), 42717.10.1038/srep42717. [PMC free article] [PubMed] [CrossRef] [Google Scholar]
35. Daina A.; Zoete V. A BOILED-Egg To Predict Gastrointestinal Absorption and Brain Penetration of Small Molecules. *ChemMedChem* 2016, 11 (11), 1117–1121. 10.1002/cmdc.201600182. [PMC free article] [PubMed] [CrossRef] [Google Scholar]
36. Szakacs G.; Varadi A.; Ozvegy-Laczka C.; Sarkadi B. The role of ABC transporters in drug absorption, distribution, metabolism, excretion and toxicity (ADME-Tox). *Drug Discovery Today* 2008, 13 (9–10), 379–93. 10.1016/j.drudis.2007.12.010. [PubMed] [CrossRef] [Google Scholar]
37. Dai Y.; Chen S.-R.; Chai L.; Zhao J.; Wang Y.; Wang Y. Overview of pharmacological activities of Andrographis paniculata and its major compound andrographolide. *Crit. Rev. Food Sci. Nutr.* 2019, 59 (sup1), S17–S29. 10.1080/10408398.2018.1501657. [PubMed] [CrossRef] [Google Scholar]
38. Jarukamjorn K.; Nemoto N. Pharmacological Aspects of *Andrographis paniculata* on Health and Its Major Diterpenoid Constituent Andrographolide. *J. Health Sci.* 2008, 54 (4), 370–381. 10.1248/jhs.54.370. [CrossRef] [Google Scholar]
39. Mussard E.; Cesaro A.; Lespessailles E.; Legrain B.; Berteina-Raboin S.; Toumi H. Andrographolide, A Natural Antioxidant: An Update. *Antioxidants* 2019, 8 (12), 571.10.3390/antiox8120571. [PMC free article] [PubMed] [CrossRef] [Google Scholar]
40. Wintachai P.; Kaur P.; Lee R. C.; Ramphan S.; Kuadkitkan A.; Wikan N.; Ubol S.; Roytrakul S.; Chu J. J.; Smith D. R. Activity of andrographolide against chikungunya virus infection. *Sci. Rep.* 2015, 5 (1), 14179.10.1038/srep14179. [PMC free article] [PubMed] [CrossRef] [Google Scholar]
41. Akbar S. Andrographis paniculata: a review of pharmacological activities and clinical effects. *Altern. Med. Rev.* 2011, 16 (1), 66–77. [PubMed] [Google Scholar]
42. Mishra K.; Dash A. P.; Dey N. Andrographolide: A Novel Antimalarial Diterpene Lactone Compound from *Andrographis paniculata* and Its Interaction with Curcumin and Artesunate. *J. Trop. Med.* 2011, 2011, 5795. [PMC free article] [PubMed] [Google Scholar]
43. Chen J. X.; Xue H. J.; Ye W. C.; Fang B. H.; Liu Y. H.; Yuan S. H.; Yu P.; Wang Y. Q. Activity of andrographolide and its derivatives against influenza virus in vivo and in vitro. *Biol. Pharm. Bull.* 2009, 32 (8), 1385–91. 10.1248/bpb.32.1385. [PubMed] [CrossRef] [Google Scholar]

44. Lee J. C.; Tseng C. K.; Young K. C.; Sun H. Y.; Wang S. W.; Chen W. C.; Lin C. K.; Wu Y. H. Andrographolide exerts anti-hepatitis C virus activity by up-regulating haeme oxygenase-1 via the p38 MAPK/Nrf2 pathway in human hepatoma cells. *British journal of pharmacology* 2014, 171 (1), 237–52. 10.1111/bph.12440. [PMC free article] [PubMed] [CrossRef] [Google Scholar]
45. Reddy V. L.; Reddy S. M.; Ravikanth V.; Krishnaiah P.; Goud T. V.; Rao T. P.; Ram T. S.; Gonnade R. G.; Bhadbhade M.; Venkateswarlu Y. A new bis-andrographolide ether from Andrographis paniculata nees and evaluation of anti-HIV activity. *Nat. Prod. Res.* 2005, 19 (3), 223–30. 10.1080/14786410410001709197. [PubMed] [CrossRef] [Google Scholar]
46. Chen H.; Ma Y. B.; Huang X. Y.; Geng C. A.; Zhao Y.; Wang L. J.; Guo R. H.; Liang W. J.; Zhang X. M.; Chen J. J. Synthesis, structure-activity relationships and biological evaluation of dehydroandrographolide and andrographolide derivatives as novel anti-hepatitis B virus agents. *Bioorg. Med. Chem. Lett.* 2014, 24 (10), 2353–9. 10.1016/j.bmcl.2014.03.060. [PubMed] [CrossRef] [Google Scholar]
47. Seubsasana S.; Pientong C.; Ekalaksananan T.; Thongchai S.; Aromdee C. A potential andrographolide analogue against the replication of herpes simplex virus type 1 in Vero cells. *Med. Chem.* 2011, 7 (3), 237–44. 10.2174/157340611795564268. [PubMed] [CrossRef] [Google Scholar]
48. Lin T. P.; Chen S. Y.; Duh P. D.; Chang L. K.; Liu Y. N. Inhibition of the epstein-barr virus lytic cycle by andrographolide. *Biol. Pharm. Bull.* 2008, 31 (11), 2018–23. 10.1248/bpb.31.2018. [PubMed] [CrossRef] [Google Scholar]
49. Ekalaksananan T.; Sookmai W.; Fangkham S.; Pientong C.; Aromdee C.; Seubsasana S.; Kongyingyoes B. Activity of Andrographolide and Its Derivatives on HPV16 Pseudovirus Infection and Viral Oncogene Expression in Cervical Carcinoma Cells. *Nutr. Cancer* 2015, 67 (4), 687–96. 10.1080/01635581.2015.1019630. [PubMed] [CrossRef] [Google Scholar]
50. Maurya V. K.; Kumar S.; Prasad A. K.; Bhatt M. L. B.; Saxena S. K. Structure-based drug designing for potential antiviral activity of selected natural products from Ayurveda against SARS-CoV-2 spike glycoprotein and its cellular receptor. *Virus Disease* 2020, 31 (2), 179–193. 10.1007/s13337-020-00598-8. [PMC free article] [PubMed] [CrossRef] [Google Scholar]
51. Kanjanasirirat P.; Suksatu A.; Manopwisedjaroen S.; Munyoo B.; Tuchinda P.; Jearawuttanakul K.; Seemakhan S.; Charoensutthivarakul S.; Wongtrakoongate P.; Rangkasenee N.; Pitiporn S.; Waranuch N.; Chabang N.; Khemawoot P.; Sa-Ngiamsuntorn K.; Pewkliang Y.; Thongsri P.; Chutipongtanate S.; Hongeng S.; Borwornpinyo S.; Thitithanyanont A. High-content screening of Thai medicinal plants reveals Boesenbergia rotunda extract and its component Panduratin A as anti-SARS-CoV-2 agents. *Sci. Rep.* 2020, 10 (1), 19963.10.1038/s41598-020-77003-3. [PMC free article] [PubMed] [CrossRef] [Google Scholar]
52. Asprea M.; Tatini F.; Piazzini V.; Rossi F.; Bergonzi M. C.; Bilia A. R. Stable, Monodisperse, and Highly Cell-Permeating Nanocochleates from Natural Soy Lecithin Liposomes. *Pharmaceutics* 2019, 11 (1), 34.10.3390/pharmaceutics11010034. [PMC free article] [PubMed] [CrossRef] [Google Scholar]
53. Chen H. W.; Huang C. S.; Li C. C.; Lin A. H.; Huang Y. J.; Wang T. S.; Yao H. T.; Lii C. K. Bioavailability of andrographolide and protection against carbon tetrachloride-induced oxidative damage in rats. *Toxicol. Appl. Pharmacol.* 2014, 280 (1), 1–9. 10.1016/j.taap.2014.07.024. [PubMed] [CrossRef] [Google Scholar]
54. Ren K.; Zhang Z.; Li Y.; Liu J.; Zhao D.; Zhao Y.; Gong T. Physicochemical characteristics and oral bioavailability of andrographolide complexed with hydroxypropyl-bete-cyclodextrin. *Die Pharmazie International J. Pharm. Sci.* 2009, 64 (8), 515–520. [PubMed] [Google Scholar]
55. Bothiraja C.; Shinde M. B.; Rajalakshmi S.; Pawar A. P. Evaluation of molecular pharmaceutical and in-vivo properties of spray-dried isolated andrographolide—PVP. *J. Pharm. Pharmacol.*

2010, 61 (11), 1465–1472. 10.1211/jpp.61.11.0005. [PubMed] [CrossRef] [Google Scholar]

56. Yen C. C.; Chen Y. C.; Wu M. T.; Wang C. C.; Wu Y. T. Nanoemulsion as a strategy for improving the oral bioavailability and anti-inflammatory activity of andrographolide. *Int. J. Nanomed.* 2018, 13, 669–680. 10.2147/IJN.S154824. [PMC free article] [PubMed] [CrossRef] [Google Scholar]
57. Sa-Ngiamsuntorn K.; Wongkajornsilp A.; Kasetsinsombat K.; Duangsa-Ard S.; Nuntakarn L.; Borwornpinyo S.; Akarasereenont P.; Limsrichamrern S.; Hongeng S. Upregulation of CYP 450s expression of immortalized hepatocyte-like cells derived from mesenchymal stem cells by enzyme inducers. *BMC Biotechnol.* 2011, 11 (1), 89.10.1186/1472-6750-11-89. [PMC free article] [PubMed] [CrossRef] [Google Scholar]
58. Pewkliang Y.; Rungin S.; Lerdpanyangam K.; Duangmanee A.; Kanjanasirirat P.; Suthivanich P.; Sa-Ngiamsuntorn K.; Borwornpinyo S.; Sattabongkot J.; Patrapuvich R.; Hongeng S. A novel immortalized hepatocyte-like cell line (imHC) supports in vitro liver stage development of the human malarial parasite Plasmodium vivax. *Malar. J.* 2018, 17 (1), 50.10.1186/s12936-018-2198-4. [PMC free article] [PubMed] [CrossRef] [Google Scholar]
59. Sa-Ngiamsuntorn K.; Thongsri P.; Pewkliang Y.; Wongkajornsilp A.; Kongsomboonchoke P.; Suthivanich P.; Borwornpinyo S.; Hongeng S. An Immortalized Hepatocyte-like Cell Line (imHC) Accommodated Complete Viral Lifecycle, Viral Persistence Form, cccDNA and Eventual Spreading of a Clinically-Isolated HBV. *Viruses* 2019, 11 (10), 952.10.3390/v11100952. [PMC free article] [PubMed] [CrossRef] [Google Scholar]
60. Reed L. J.; Muench H. A simple method of estimating fifty per cent endpoints. *Am. J. Epidemiol.* 1938, 27 (3), 493–497. 10.1093/oxfordjournals.aje.a118408. [CrossRef] [Google Scholar]
61. Najib Y.; Wan-Azemin A.; Dharmaraj S.; Suryati K. Phytochemical Screening and Prophylactic Antibacterial Effects of Andrographis Paniculata Extracts from Kemaman, Malaysia. *J. Nat. Sci. Res.* 2015, 5, 67–72. [Google Scholar]
62. Sani Y. N.; Danladi S.; Wan-Azemin A.; Us M. R.; Mohd K. S.; Dharmaraj S. Effects of extracting solvents on total phenolic content, total flavonoid content and anti-oxidant activity of Andrographis paniculata from Kemaman, Malaysia. *Res. J. Pharm, Biol. Chem. Sci.* 2015, 6, 1397–1404. [Google Scholar]